

## A Property of Stick-Slip Friction Models which Promotes Limit Cycle Generation

Clark J. Radcliffe  
Associate Professor

Steve C. Southward  
Graduate Student

Department of Mechanical Engineering  
Michigan State University  
East Lansing, Michigan 48824

### Abstract

The effects of various "Stick-Slip" friction models on Proportional+Integral+Derivative (PID) controller stability for a simple system are investigated. Some of the more common models lack the ability to produce the limit cycles commonly observed for servos subject to stick-slip friction. A property of stick-slip models is identified which promotes limit cycle generation, and the effects are demonstrated through numerical simulations. This property is shown to be required for a stick-slip friction model to be useful in predicting limit cycle behavior in the simplest systems under PID control. Models lacking this property may lead to the inaccurate prediction of system dynamics.

### Introduction

Stick-Slip friction exists in virtually every mechanical system and its presence can appreciably affect the system dynamics. This nonlinear phenomenon has caused great difficulty in both modelling and control. Although a control design engineer can choose to design the system to reduce the effects of this type of friction, it is always present to some degree. Precise position control tasks such as those found in robotics applications (Gogoussis and Donath, 1987; Kubo and Tomizuka, 1986), or in X-Y tables (Yang and Tomizuka, 1987), are examples of systems affected by this problem. One of the most important effects of this type of friction is its ability to cause undesirable limit cycles in control applications (Townsend and Salisbury, 1987).

Many models for "Stick-Slip" friction are available for use in dynamic simulations or analysis (Kolston, 1988; Canudas, et al., 1987; Shaw, 1986). In choosing a suitable model, there is a trade-off between simplicity and effectiveness in predicting the system dynamics. Simulated system dynamics using a stick-slip friction model should accurately represent the dynamics observed in a real system. This paper investigates what properties of stick-slip models lead to limit cycle generation. A specific property is presented whereby friction models can be easily classified as to their ability to produce limit cycles. Friction models from three representative classes have been tested under the same operating conditions in a simple one-degree-of-freedom (1-DOF) system with a Proportional+Integral+Derivative (PID) control scheme. Numerically simulated state trajectories from these non-linear models are then used to determine which models can predict a limit cycle response.

### System Models

A 1-DOF system, sufficient to provide the required dynamics for this limit cycle investigation, is a mass constrained to move in one dimension with stick-slip friction,  $F_d$  (Fig. 1). The control force acting parallel to the

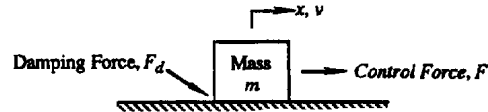


Figure 1. The 1-DOF conceptual stick-slip mass system used to investigate models of stick-slip friction.

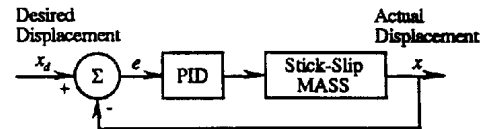


Figure 2. Block Diagram of PID control system incorporating stick-slip mass system.

direction of motion is governed by a Proportional-Derivative (PD) or a PID control law. The general system equation for PID control is

$$m\ddot{x} + F_d = K_p e + K_d \dot{e} + K_i \int_0^t e dt \quad (1)$$

where the actuating error,  $e = x_d - x$ . The regulator problem is the simplest controller action which can exhibit limit cycles, and without loss of generality one can set the desired states to be at the origin (i.e.  $x_d(t) = 0$  and  $\dot{x}_d(t) = 0 \forall t \geq t_0$ ). This system is linear with the exception of the Coulomb damping force  $F_d$ . The system equations can be written in state-space canonical form for  $x_d(t) = 0$  as

$$\begin{bmatrix} \dot{y} \\ \dot{x} \\ \dot{v} \end{bmatrix} = \begin{bmatrix} 0 & 1 & 0 \\ 0 & 0 & 1 \\ -\frac{K_i}{m} & -\frac{K_p}{m} & -\frac{K_d}{m} \end{bmatrix} \begin{bmatrix} y \\ x \\ v \end{bmatrix} - \begin{bmatrix} 0 \\ 0 \\ \frac{F_d}{m} \end{bmatrix} \quad (2)$$

with the identities  $v = \dot{x}$  and  $y = -\int_0^t e dt$ .

Karnopp (1985) introduced a model for stick-slip friction that not only allows for the computation of the damping force during sticking and slipping motions, but considers the problem of integration algorithm stability associated with near-zero velocity force computation. The conceptual stick-slip friction model is achieved with equation (3) only in the limit as  $\alpha \rightarrow 0$ . A reformulation of Karnopp's model can be constructed as the following

$$F_d = F_{slip}(v)\lambda_\alpha(v) + F_{stick}(F_s)(1 - \lambda_\alpha(v)) \quad (3a)$$

$$\lambda_\alpha(v) = \begin{cases} 1 & |v| > \alpha \\ 0 & |v| \leq \alpha \end{cases}, \alpha > 0 \quad (3b)$$

The "sticking" function ( $F_{stick}$ ) provides values of the damping force at zero velocity, or for this model when the velocity is within  $\alpha$  of zero. The static friction force threshold is given by  $F_s$ .

$$F_{stick}(F_s) = \begin{cases} F_s & F_s \geq F_s \\ F_s & |F_s| < F_s, F_s > 0 \\ -F_s & F_s \leq -F_s \end{cases} \quad (4)$$

Implicit in this definition is the assumption that the positive and negative static friction levels are equal in magnitude and they are also assumed to be constant. The reaction force,  $F_r$ , is the equilibrium force required by the damping mechanism to keep the mass at rest when the velocity becomes zero. For the PID control system in (2), the reaction force

$$F_r = -[K_d v + K_p x + K_y] \quad (5)$$

The "slipping" function,  $F_{slip}(v)$  provides values of the damping force at non-zero velocities, and is what would normally be referred to as the friction model. This paper will look at three general classes of friction model or "slipping" functions (Fig. 3). For simplicity, the slipping function is assumed to be odd. The three classes of stick-slip friction models (Fig. 3) were chosen to represent most of the standard models found in the literature today (Craig, 1988; Gogoussis and Donath, 1987; Canudas, et al., 1987). A viscous damping term is included in each model since it is a common linear damping model.

The characteristic form of the slipping force  $F_{slip}(v)$ , will be shown to cause limit cycle response and is the primary subject of this paper. The slipping force is also assumed to

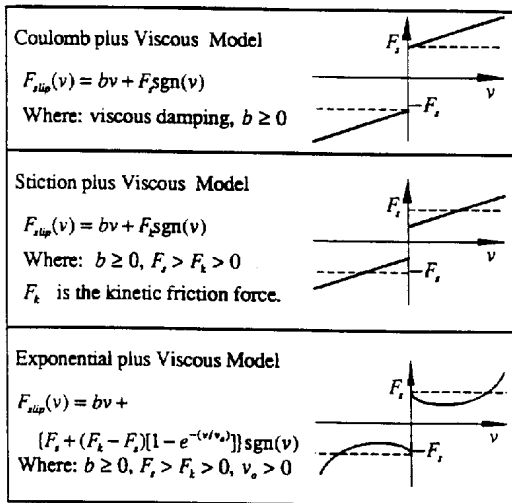


Figure 3. Three classes of slipping friction models under investigation with examples of each.

be dissipative thus requiring that

$$(vF_{slip}) \geq 0 \quad \forall v \quad (6)$$

The numerical implementation of  $F_{slip}(v)$  requires that it be separated into two parts:  $F_d^{(+)}(v)$  which is defined only for positive velocity, and  $F_d^{(-)}(v)$  which is defined only for negative velocity, i.e.

$$F_{slip}(v) = F_d^{(+)}(v - \epsilon)\mu(v) + F_d^{(-)}(v + \epsilon)\mu(-v) \quad (7)$$

where  $\mu(\cdot)$  is the right-continuous heavyside step function.

### The PD Control Space

For the system given in (2-7), under PD control, the y-coordinate is not required and solution trajectories exist in a two-dimensional phase space with coordinates  $(x, v)$ . In this space, there exists a set of equilibrium points where all derivatives are zero. From (2) with  $K_v = 0$ , equilibrium is achieved when  $F_d(v = 0) = -K_p x$ . From (3-5) we have zero acceleration, if and only if  $|K_p x| \leq F_s$ . Defining two constants ( $x_L$  and  $x_H$ ), the set of equilibrium points for the PD phase space (Fig. 4) can be written as:  $E_{PD} = \{(x, v) \mid v = 0, x_L \leq x \leq x_H\}$  where:

$$x_L = -\left(\frac{F_s}{K_p}\right), \quad x_H = \left(\frac{F_s}{K_p}\right) \quad (8)$$

The PD-space equilibrium set is an invariant set and Lyapunov's direct method for stability of invariant sets can be employed to verify the stability of  $E_{PD}$  (Hahn, 1963, and 1967). If the PD control gains are chosen to stabilize the undamped system, then with the proper choice of a Lyapunov function, it can be shown that the equilibrium set  $E_{PD}$  is globally asymptotically stable. Every trajectory will terminate with zero velocity and a bounded steady-state error. More importantly, no limit cycles can exist in the PD control space for damping functions of the form (3-7) under the above assumptions. Simulations show that trajectories spiral clockwise and verify the stability of  $E_{PD}$  (Fig. 4).

There are only two trajectories in the PD space that take the system directly to the origin. The steady-state error bounds ( $x_L$  and  $x_H$ ) can be reduced by increasing the proportional gain  $K_p$ , as indicated by (8), but at the expense of large control forces far away from the origin.

### The PID Control Space

The PID control solution space for (2-7) is three dimensional with state coordinates  $(y, x, v)$ . There are several subspaces in this phase space which have interesting features. The first subspace is the equilibrium set, which is the set of all coordinates where all derivatives are zero. The solution of (2) with zero derivatives yields  $F_d(v = 0) = -K_y y$ . Therefore from (2-5) the system is in equilibrium if and only if  $|K_y y| \leq F_s$ . Defining two new constants ( $y_L$  and  $y_H$ ), the set

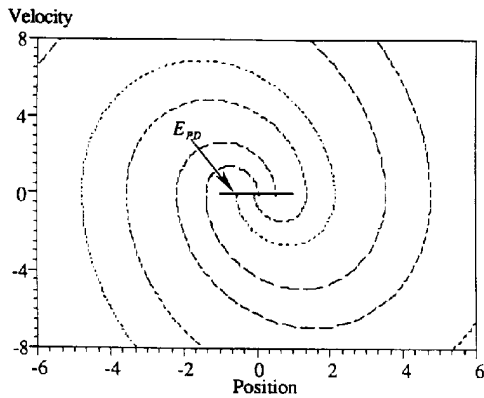


Figure 4. Typical PD Phase Portrait showing trajectories spiraling clockwise and terminating in  $E_{PD}$ .

of equilibrium points for the PID phase space can be written as:  $E_{PID} = \{(y, x, v) | x = 0, v = 0, y_L \leq y \leq y_H\}$ , where

$$y_L = -\left(\frac{F_s}{K_i}\right), \quad y_H = \left(\frac{F_s}{K_i}\right) \quad (9)$$

Notice the difference between this set and the previous set  $E_{PD}$ . Even though it is not a single point set, any trajectories which end in  $E_{PID}$  reach both the desired states  $x_d$  and  $v_d$ . Unlike the stable PD equilibrium set, this equilibrium set can be unstable. As will be shown below, for some types of friction models, trajectories near the set  $E_{PID}$  diverge away from the set to a stable limit cycle.

There exists a subspace where the system dynamics are reduced to first order. In the  $x$ - $y$  plane,  $v = 0$  and from (3-5) we have zero acceleration if and only if  $|K_i y| \leq F_s$ . Using the previous definitions (8) and (9), one can write the following equivalent expressions

$$\dot{v} = 0 \Leftrightarrow \begin{cases} y_L \leq (y + (K_p / K_i)x) \leq y_H \\ x_L \leq (x + (K_i / K_p)y) \leq x_H \end{cases} \quad (10)$$

These inequalities define a band in the  $x$ - $y$  plane shown in Figure 5. This "sticking" band can be defined in a way that is similar to the definition of the equilibrium set as the union of two sets;  $S = S_1 \cup S_2$ , where  $S_1 = \{(y, v, x) | y_L \leq (y + (K_p / K_i)x) \leq y_H, v = 0, x > 0\}$ , and  $S_2 = \{(y, v, x) | y_L \leq (y + (K_p / K_i)x) \leq y_H, v = 0, x < 0\}$ . Inside this band, the system dynamics (2) are reduced to first order in the state  $y$ . Trajectories in  $S$  represent "sticking" trajectories where the mass remains stationary until the force due to the integral of the error builds up to a level greater than the static friction force. Given an initial condition  $(y_{po}, x_{po}, v_{po}) \in S$  at time  $t_{po}$ , state solutions are given by

$$\begin{bmatrix} y_s(t) \\ x_s(t) \\ v_s(t) \end{bmatrix} = \begin{bmatrix} x_{po}(t - t_{po}) + y_{po} \\ x_{po} \\ 0 \end{bmatrix} \quad t_{po} \leq t \leq t_{sf}$$

The mass will break free at time  $t_{sf}$  given by

$$t_{sf} = t_{po} + (1 / x_{po}) \begin{cases} y_H - (y_{po} + (K_p / K_i)x_{po}) & x_{po} > 0 \\ y_L - (y_{po} + (K_p / K_i)x_{po}) & x_{po} < 0 \end{cases}$$

Trajectories in  $S$  are parallel to the  $y$ -axis, and their direction is dependent on the sign of  $x$ , (Fig. 5). These trajectories show the equilibrium,  $E_{PID}$  to be unstable for small perturbations in  $x$  and  $y$ .

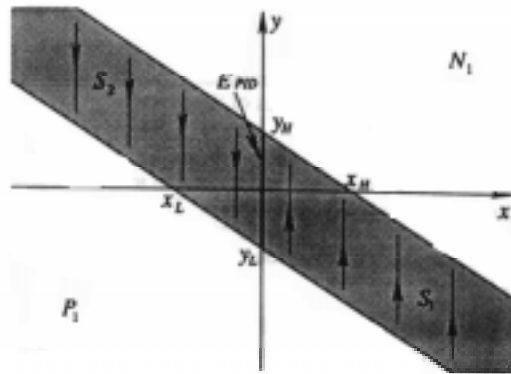


Figure 5. Parallel trajectories inside the sticking band  $S$  have zero acceleration until they reach the border.

The remainder of the 3-dimensional PID control space can be divided up into two regions  $N$  and  $P$ , characterized by the sign of the velocity component of state trajectories inside each region. These regions are:  $P = P_1 \cup P_2$ , where  $P_1 = \{(y, v, x) | y_L \geq (y + (K_p / K_i)x), v = 0\}$ , and  $P_2 = \{(y, v, x) | v > 0\}$ . The rest of the space is similarly defined as:  $N = N_1 \cup N_2$ , where  $N_1 = \{(y, v, x) | y_H \leq (y + (K_p / K_i)x), v = 0\}$ , and  $N_2 = \{(y, v, x) | v < 0\}$ . From (4) and (5), we have:  $(y, x, v) \in N_1 \Rightarrow (dv/dt) \leq 0$  and  $(y, x, v) \in P_1 \Rightarrow (dv/dt) \geq 0$ . All initial conditions  $(y_{po}, v_{po}, x_{po}) \in P$  at time  $t_{po}$  have trajectories with non-negative velocity component until time  $t_{sf}$ , and all initial conditions  $(y_{no}, v_{no}, x_{no}) \in N$  at time  $t_{no}$  have trajectories with non-positive velocity component until time  $t_{sf}$ . The final times are the first time after  $t_{po}$  or  $t_{no}$  where the velocity is zero, i.e. in  $P$ :  $v_p(t_{sf}) = 0$  and  $v_p(t) \neq 0 \quad \forall t \in (t_{po}, t_{sf})$ , and in  $N$ :  $v_n(t_{sf}) = 0$  and  $v_n(t) \neq 0 \quad \forall t \in (t_{no}, t_{sf})$ .

This sticking band  $S$  plays an important role in the generation of limit cycles in the PID space. The  $x$ -coordinate of a point in  $S$  physically represents the displacement of the mass away from the origin (the desired position) where the mass remains stuck until the integral force term breaks it free. Near the origin, all trajectories in  $S_1$  enter  $N$  and then enter  $S_2$ . Also near the origin, all trajectories in  $S_2$  enter  $P$ .

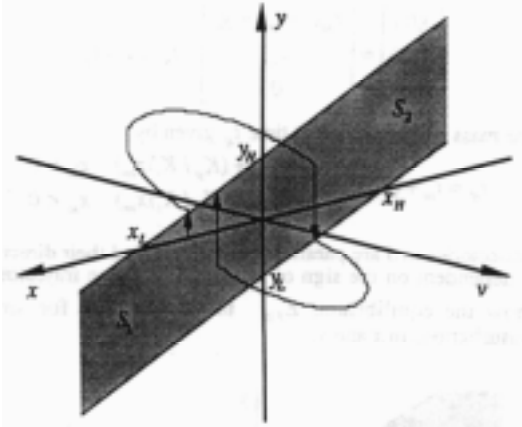


Figure 6. Typical PID trajectory showing sticking on both sides of the origin.

and similarly re-enter  $S_1$ . Physically, the mass is stuck on one side of the origin until the force due to the integral term builds up enough to break it free. It then overshoots the origin and sticks on the other side. A similar process is repeated on the return motion. A typical trajectory is shown in Figure 6.

Existence and stability of a limit cycle for a given system can be determined through the construction and examination of mappings of trajectories from points in  $S_1$  to  $S_2$  and then back to  $S_1$ . In fact, existence and stability of limit cycle trajectories can be determined from mappings of an  $x$ -coordinate of a point in  $S_1$  into the subsequent  $x$ -coordinate in  $S_1$ . Simulation data of  $x$ -coordinates in  $S_1$  mapped back into  $S_1$  can be used to numerically construct a continuous iteration function for a given set of system parameters. Limit cycles will appear as fixed points of these iteration map functions. The contraction mapping theorem can then be applied to prove the existence of fixed points (Vidyasagar, 1978). This will be the method employed here to study various types of "Stick-Slip" friction models.

**Simulation**

Equations (3-7) along with the models for  $F_{slip}(v)$  in Figure 3 completely define the friction force. The following set defines the characteristic property of the assumed symmetric slipping force models investigated in this paper

$$U = \{F_{slip}(v) | \exists v^* > 0 \ni F_{slip}(v) < F_s^+ \forall v \in (0, v^*)\} \quad (11)$$

If a slipping force model belongs to the set  $U$ , it will take on values which are less than the static friction level in a region near zero velocity. It will be shown that models belonging to the set  $U$  will promote limit cycles in the 1-DOF system under PID control. The models from Fig. 3 yield the classifications in Table 1.

The Coulomb model always provides forces which are greater than the static friction levels therefore it is not in the set  $U$ . The Stiction model has a discontinuous drop from the static level to a non-decreasing slipping force as the velocity increases in magnitude thus it belongs in the set  $U$ . The Exponential model undergoes a continuous drop from the

Coulomb Model plus Viscous Damping	$F_{slip}(v) \notin U$
Stiction Model plus Viscous Damping	$F_{slip}(v) \in U$
Exponential Model plus Viscous damping	$F_{slip}(v) \in U$

Table 1. Classifications for each of the three stick-slip models.

Mass of block	$m = 1.0$ kg.
Static Friction force	$F_s = 4.0$ N.
Kinetic Friction force	$F_k = 2.0$ N.
Control gains	$K_p = K_d = 10.0$
	$K_i = 100.0$
Artificial Zero parameter	$\alpha = 0.001$ m/s.

Table 2. Set of constant parameters used with each simulation of the stick-slip mass system.

static level to a lower kinetic level then increases. The Exponential model, like the Stiction model is also in  $U$ .

Using the damping model examples (Fig. 3), solutions to equations (2-7) are nonlinear, and solutions are only piecewise linear for the first two classes. Since no general closed form solution exists, a numerical simulation was performed to determine the contraction mappings. Three representative examples from each class of stick-slip friction model above were numerically simulated. All cases used the set of constant parameters shown in Table 2.

Simulations were performed in double-precision on a Digital Equipment Corporation Micro-VAX, using a Hamming predictor-corrector general integration method with an initial step size of 0.001 s. For each run, a number of initial conditions inside  $S_1$  were chosen to provide an evenly distributed data set for generating the iteration functions. Each  $x_i$  is an  $x$ -coordinate in  $S_1$  and  $x_{i+1}$  is the  $x$ -coordinate for the next time the trajectory enters  $S_1$ . A second order polynomial of the form:  $x_{i+1} = (a_0 + a_1x_i + a_2x_i^2)$ , was fit through each set, and then plotted. There is an iteration function fit associated with each set of parameters.

The numerical fixed points were obtained by guessing an initial value and then iterating the function until the error between successive iterations was less than 1.0E-9. Convergence is guaranteed since the slopes are less than unity. A conservative error estimate,  $\epsilon$ , for each fixed point is obtained by using the largest absolute residual error from the curve fit to form a band around the fitted function. All data from the respective curve fit is guaranteed to be inside this band. The fixed points of the two functions defining the edges of this band are then used to determine conservative error estimates in the original fixed point. These error estimates are presented with each of the fixed point estimates.

For the Coulomb plus Viscous friction models, the three representative cases were obtained by varying the viscous damping coefficient.  $b$  (Table 3).

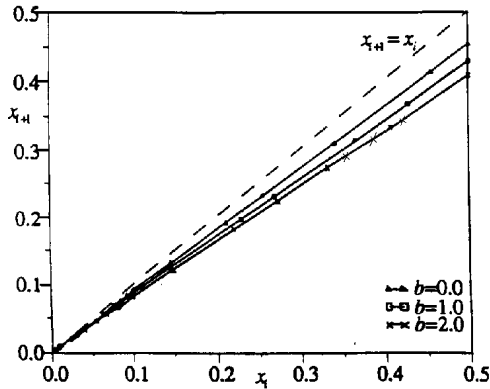


Figure 7. Coulomb plus Viscous friction model iteration functions with varying viscous damping coefficient  $b$ .

$b$	2.0	1.0	0.0
$a_0(\times 10^{-4})$	1.87	2.05	1.99
$a_1$	0.814	0.853	0.906
$a_2(\times 10^{-3})$	6.37	7.39	7.00
$(x \pm \varepsilon)(\times 10^{-3})$	$1.01 \pm 1.51$	$1.40 \pm 2.10$	$2.12 \pm 4.65$

Table 3. Coulomb plus Viscous model polynomial fit coefficients  $a_i$ ; and the corresponding fixed points  $x$ , with error estimate  $\varepsilon$ ; versus viscous damping coefficient  $b$ .

The simulation results for this class are plotted in Figure 7. Shown on this plot is the line:  $x_{i+1} = x_i$ , along with the fitted iteration functions for the three test cases. A fixed point occurs whenever an iteration function crosses the  $x_{i+1} = x_i$  line. All three test cases (Fig. 7) have a fixed point at the origin, i.e.  $x_{i+1} = x_i \Leftrightarrow x_i = 0$ . The intercepts ( $a_0$ ) of the polynomials from the curve fit, as seen from table 3, indicate that no limit cycles exist for this class of models. Within the accuracy of the simulation, all trajectories eventually converge to the origin (Table 3).

For the Stiction plus Viscous friction models, the three representative test cases were similarly obtained by varying the viscous damping coefficient,  $b$  (Table 4). The simulation results for the Stiction plus Viscous friction models are plotted in Figure 8. For each of these three test cases, there is a non-zero fixed point which is different for each case. The actual fixed points can be found in Table 4 for each of the cases. As seen from Figure 8, and verified with the polynomial curve fit, the local slopes of these iteration functions near their fixed points are always less than unity. The contraction mapping theorem can be used to prove that these fixed points are all stable (Vidyasagar, 1978). For example when  $b=2.0$  (N-s/m), there will be a stable limit cycle with amplitude  $x = 0.136$  m.

For the Exponential plus Viscous friction models, the three representative cases were obtained by varying both the viscous damping coefficient  $b$ , and the velocity constant  $v_0$ , (Table 5).

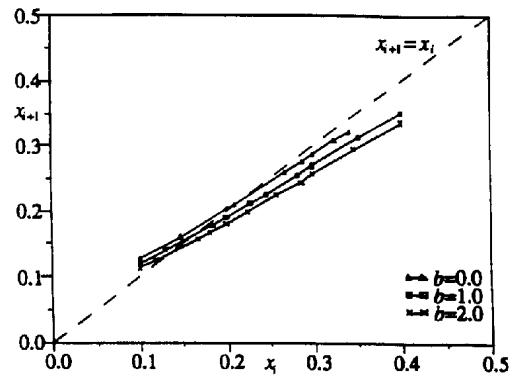


Figure 8. Stiction plus Viscous friction model iteration functions with varying viscous damping coefficient  $b$ .

$b$	2.0	1.0	0.0
$a_0$	0.0452	0.0489	0.0565
$a_1$	0.635	0.663	0.669
$a_2$	0.236	0.246	0.334
$x \pm \varepsilon$	$0.136 \pm 0.003$	$0.165 \pm 0.004$	$0.219 \pm 0.006$

Table 4. Stiction plus Viscous model polynomial fit coefficients  $a_i$ ; and the corresponding fixed points  $x$ , with error estimate  $\varepsilon$ ; versus viscous damping coefficient  $b$ .

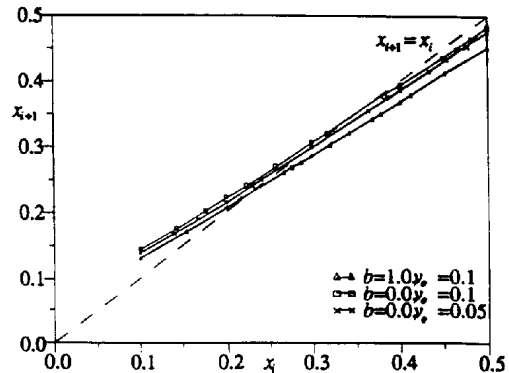


Figure 9. Exponential plus Viscous friction model iteration functions with varying viscous damping coefficient  $b$ , and velocity constant  $v_0$ .

$b$	0.0	0.0	1.0
$v_0$	0.05	0.10	0.10
$a_0$	0.0628	0.0638	0.0553
$a_1$	0.732	0.767	0.735
$a_2$	0.190	0.138	0.120
$x \pm \varepsilon$	$0.297 \pm 0.008$	$0.343 \pm 0.004$	$0.233 \pm 0.002$

Table 5. Exponential plus Viscous model polynomial fit coefficients  $a_i$ ; and the corresponding fixed points  $x$ , with error estimate  $\varepsilon$ ; versus viscous damping coefficient  $b$ , and velocity constant  $v_0$ .

The Exponential plus Viscous friction model results (Fig. 9) also indicate the existence and stability of limit cycles but at larger amplitudes than those for Stiction (Table 5). The local slopes near the corresponding fixed points are less than unity, so these fixed points are all stable.

From the plots in Figure 7, and the Table 3 data, as viscous damping is decreased, the slope of the iteration function increases, and the fixed point remains near zero. From Figure 8, and Table 4, as the viscous damping is decreased, the fixed point of the iteration function increases. This observation is important since fast convergence to the fixed point (stable limit cycle) is obtained when the slope of the iteration function near a fixed point is close to zero. Since the cases investigated here all have slopes near unity, the convergence is slow. Raising the iteration functions further away from the  $x$ -axis (i.e. increasing  $a_0$ ) has the effect of increasing the amplitude of the limit cycle. The presence of viscous damping can therefore help stabilize by either decreasing convergence times as in the case of Coulomb models, or by reducing the limit cycle amplitude as in the case of Stiction and Exponential models.

### Conclusions

A suitable stick-slip friction model for control system simulation or analysis, which can provide limit cycle solutions, is required for investigating limit cycles reported in practice. Our results indicate that the common Coulomb friction model should not be used in this case. To allow limit cycle response in the one degree of freedom model investigated here, the damping function must drop for non-zero velocity from the static friction force level, either continuously, e.g. Exponential models, or discontinuously, e.g. Stiction models, to a lower value than the static level.

The above results can also be interpreted for qualitative characterizations of the damping present in a real system. If a real 1-DOF system exhibits limit cycle behavior under PID control, then the stick-slip friction present in the system must have the same properties as either the Stiction or Exponential models as defined in Table 1. On the other hand, if the system under PID control converges to the desired equilibrium, the friction present must have the same properties of the Coulomb models (Table 1).

The Coulomb models are qualitatively different from the Stiction or Exponential models in that there is no drop in slipping friction force from the static level. This difference has been shown to provide a difference in the richness of the dynamic solutions for a 1-DOF system. Great care must be taken to insure that the friction model can indeed provide the proper qualitative dynamics. This is particularly important for simulations which are used to test for stability properties of new control schemes.

For models belonging to any of the three classes, the PD control scheme applied to the simple 1-DOF system is stable with respect to the equilibrium set  $E_{PD}$ . Adding integral control de-stabilizes the same system with friction modelled by the Stiction or Exponential models. Proper control system design requires stick-slip models which are actually able to predict this limit cycle behavior.

### Acknowledgement

The authors are grateful to Dr. Steve Shaw for his assistance.

### References

- Canudas, C., Astrom, K., and Braun, K., 1987, "Adaptive Friction Compensation in DC Motor Drives," *IEEE Journal of Robotics and Automation*, Vol. RA-3, No. 6, Dec., pp. 681-685.
- Craig, J., 1988, *Adaptive Control of Mechanical Manipulators*, Addison-Wesley Publishing Company Inc.
- Gogoussis, A., and Donath, M., 1987, "Coulomb Friction Joint and Drive Effects in Robot Mechanisms," *IEEE Intl. Conf. on Robotics & Automation*, pp. 828-836.
- Hahn, W., 1963, *Theory and Application of Liapunov's Direct Method*, Prentice-Hall, Englewood Cliffs, New Jersey, pp. 75-78.
- Hahn, W., 1967, *Stability of Motion*, Springer-Verlag, New York Inc., pp. 166-224.
- Karnopp, D., 1985, "Computer Simulation of Stick-Slip Friction in Mechanical Dynamic Systems," *ASME Journal of Dynamic Systems, Measurement, and Control*, Vol. 107, pp. 100-103.
- Kolston, P., 1988, "Modeling Mechanical Stick-Slip Friction Using Electrical Circuit Analysis," *ASME Journal of Dynamic Systems, Measurement, and Control*, Vol. 110, Dec., pp. 440-443.
- Kubo, T., and Tomizuka, M., 1986, "Application of Nonlinear Friction Compensation to Robot Arm Control," *IEEE International Conference on Robotics and Automation*, Vol. 2, pp. 722-727.
- Shaw, S., 1986, "On the Dynamic Response of a System with Dry Friction," *Journal of Sound and Vibration*, Vol. 108(2), pp. 305-325.
- Townsend, W., and Salisbury, J.K., 1987, "The Effect of Coulomb Friction and Stiction on Force Control," *IEEE International Conference on Robotics and Automation*, Vol. 2, pp. 883-889.
- Vidvasagar, M., 1978, *Nonlinear Systems Analysis*, Prentice-Hall, Englewood Cliffs, New Jersey.
- Yang, S., and Tomizuka, M., 1987, "Adaptive Pulse Width Control for Precise Positioning Under Influence of Stiction and Coulomb Friction," *ASME J. Dyn. Sys. Meas. Control*, Vol 110, No 3, pp. 221-227, Sept. 1988.